Available online at www.sciencedirect.com

Food and Bioproducts Processing

journal homepage: www.elsevier.com/locate/fbp

Comparative study of the production of cellulose nanofibers from agro-industrial waste streams of *Salicornia ramosissima* by acid and enzymatic treatment

Alexandre R. Lima[a,b], *Nathana L. Cristofoli*[a], *Ana M. Rosa da Costa*[c], *Jorge A. Saraiva*[b], *Margarida C. Vieira*[a,d,*]

[a] *MED–Mediterranean Institute for Agriculture, Environment and Development & CHANGE–Global Change and Sustainability Institute, Faculty of Sciences and Technology, Universidade do Algarve, Campus de Gambelas, 8005-139 Faro, Portugal*

[b] *LAQV–REQUIMTE, Department of Chemistry, University of Aveiro, 3810-193 Aveiro, Portugal*

[c] *CIQA–Algarve Chemistry Research Centre, Department of Chemistry and Pharmacy, Universidade do Algarve, Campus de Gambelas, 8005-139 Faro, Portugal*

[d] *ISE–High Institute of Engineering, Department of Food Engineering, Universidade do Algarve, Campus da Penha, 8005-139 Faro, Portugal*

ARTICLE INFO

Article history:
Received 13 April 2022
Received in revised form
14 November 2022
Accepted 28 November 2022
Available online 2 December 2022

Keywords:
Salicornia ramosissima
Agro-industrial waste
Enzymatic hydrolysis
Cellulose nanofibers
Biopolymer

ABSTRACT

The study of the suitability of two isolation processes to produce cellulose nanofibers (CNFs) from *Salicornia ramosissima* waste, with potential applicability as a reinforcing agent of polymeric composites was carried out. To separate the cellulose fibrils from the cell wall and obtain CNFs an alkaline treatment was applied followed by a bleaching treatment and, the insoluble residue was next hydrolyzed by either an acid treatment (AT) or an enzyme treatment (ET). SEM and TEM images indicated fiber exposure caused by both treatments. The diameter, length, aspect ratio, and polydispersity index, were measured for both CNFs. CNF (ET) showed high zeta potential values suggesting that ET produces more electrically stable and thinner nanofibers. The FTIR spectra revealed that both treatments effectively removed the amorphous components allowing the CNFs isolation, and XRD patterns evidenced the increase in the degree of crystallinity of both CNFs. Nonetheless, CNF(AT) presented a lower mechanical resistance due to its smaller particle size, compared to the CNF(ET). In summary, the (ET) could successfully isolate CNFs from the Salicornia waste, encouraging the use of this treatment, once when compared to (AT), it does not generate toxic residues, presents mild thermal conditions, and produces CNFs with higher-value applications.

* Corresponding author at: MED–Mediterranean Institute for Agriculture, Environment and Development & CHANGE–Global Change and Sustainability Institute, Faculty of Sciences and Technology, Universidade do Algarve, Campus de Gambelas, 8005-139 Faro, Portugal.
E-mail address: mvieira@ualg.pt (M.C. Vieira).

https://doi.org/10.1016/j.fbp.2022.11.012

1. Introduction

Globally, it is estimated that one-third of all produced food is wasted or lost, caused in great part by the fruit, vegetable, and seafood industry (FAO, 2019). According to Marić et al. (2018), only Europe generates around 100 Mt of food waste and by-products per year, with 14.8% being attributed to fruit and vegetable industries. These by-products include pomace, peel, cuts, stems, bran, and seeds, with interesting functional and nutritional potential (Ayala-Zavala et al., 2011). Considering these facts, the management of agro-industrial waste is one of the issues strictly related to the goals for sustainable development (SDGs) proposed by the 2030 Agenda of the United Nations (United Nations, 2015). SDG Target 12.3 addresses the reduction of global food waste at the retail and consumer levels to half of the actual value as well as reducing food loss from post-harvest to production and distribution chains by 2030. SDG 2 by addressing the Zero hunger Goal, will be positively affected by the reduction of food waste loss as well as other SDGs that will also profit from this reduction, namely SDG 6 (sustainable water management), SDG 13 (climate change), SDG 14 (marine resources), SDG 15 (terrestrial ecosystems, forestry, biodiversity) (FAO, 2019).

The sustainable use of agri-food waste and by-products to produce value-added products, with potential application in the food, cosmetics, and pharmaceutical industries, can provide new opportunities to generate additional income for the industry (Ben-Othman et al., 2020). According to Alcántara et al. (2020), the nonedible parts of plants left in the field after harvesting, namely crop residues, are agro-industrial waste that generally has a chemical composition rich in lignocellulosic fibers, such as cellulose.

Cellulose is an abundant biopolymer well-known for being the raw material for paper production which has a regular chemical composition, it is biodegradable and renewable, but when obtained from plant materials, has a complex, physical and morphological structure (Hansson et al., 2009; Siró and Plackett, 2010). Overall, cellulose fibers are obtained from wood pulp and present characteristics of short fibers (1–5 mm), ideal for composite production with a non-specific fiber orientation due to their isotropic properties. Otherwise, they present a luminal area between 20% and 70% of the fiber cross-sectional area (Madsen and Gamstedt, 2013). Since the fibers in herbs and small plants are longer (5–30 mm), their orientation and arrangement can be controlled. In addition, they have a higher degree of crystallinity and lower luminal area, between 0% and 5%, characteristics of fibers with excellent mechanical properties (Madsen and Gamstedt, 2013; Müssig, 2010; Sorieul et al., 2016). Therefore, small plant residues provide a low-cost source of cellulose fibers that is sustainable and able to produce high-quality CNFs with added value.

Recently, there has been a growing interest in cellulose fibers for the isolation of nanocellulose. Nanocellulose is a material with versatile physicochemical properties with a wide variety of applications, but it requires specific methodologies for its isolation that must be adapted to each raw material (Ribeiro et al., 2019). Two types of nanocellulose can be isolated from the plant wall, cellulose nanocrystals (CNCs) and cellulose nanofibers (CNFs) (Abdul Khalil et al., 2014), being the latter with excellent applicability as a reinforcing agent in composite materials such as biofilms and plastic packaging. However, despite the growing market interest, nanocellulose has a high cost and has some production conditions that are unfriendly to the environment, such as acid hydrolysis with sulfuric acid (H_2SO_4) which uses high temperatures and generates toxic residues (Liu et al., 2016; Ribeiro et al., 2019).

Finding solutions to change these aspects can be decisive for the commercial success of plant materials that are good sources of nanocellulose. In this sense, several studies have proposed new techniques for nanocellulose isolation that go beyond the traditional techniques of alkaline hydrolysis, bleaching, and acid hydrolysis (Abdul Khalil et al., 2014). The enzymatic hydrolysis method, for example, keeps reasonable production yields, uses mild temperatures, reduces the production time, and does not generate toxic residues to the environment, in addition to producing nanocellulose with appealing physicochemical properties. An overview of the isolated nanocellulose types obtained by enzymatic treatment from different agro-industrial wastes and by-products as well as the enzymes used is presented in Table 1.

Cellulose enzymatic hydrolysis is a biochemical process commonly performed by an enzyme complex called cellulases. Cellulases play a predominant role as a catalyst in the hydrolysis of cellulose polysaccharide, namely polymeric cellulosic substrates, by breaking β-1,4-glycosidic bonds, and their subsequent conversion into monomeric cellulosic products (Jayasekara and Ratnayake, 2019; Singh et al., 2019). In this sense, Zhu et al. (2011) suggested a short-term enzymatic hydrolysis as a strategy to avoid cellulose degradation of the product. Overall, cellulases are divided into three main groups: endoglucanases, exoglucanases, and β-glycosidases (Henrissat and Bairoch, 1993). For complete cellulose hydrolysis, at least two enzymes of the cellulase complex must work synergistically. Endoglucanases can act directly on the amorphous regions of the cellulose chain, producing oligosaccharides of different sizes. On the other hand, exoglucanases act at the ends of the cellulose fibers producing cellobiose (cellobiohydrolases) and glucose (glucohydrolases). Finally, these cellobioses will be degraded by

Table 1 – Examples of isolated nanocellulose from agricultural residues by enzymatic treatment.

Agro-Industrial Waste	Nanocellulose	Enzyme	Reference
Banana peels	Cellulose nanofibers	Xylanase	Tibolla et al. (2014)
Cassava bagasse	Cellulose nanofibers	Amylase	Panyasiri et al. (2018)
Corncob residues	Cellulose nanofibrils; Cellulose nanoparticles	Cellulase	Xu et al. (2021)
Curauá leaves	Cellulose nanofibers	Cellulase blend	Campos et al. (2013)
Orange Peel waste	Cellulose nanofibers	Pectinase blend	Hideno et al. (2014)
Sugarcane bagasse	Cellulose nanocrystals; Cellulose nanofibrils	Cellulase blend; Xylanase	Campos et al. (2013); Pereira and Arantes (2020); Saelee et al. (2016)
Wheat straw	Lignocellulosic nanofibers	Cellulase	Espinosa et al. (2019)

producing glucose monomers by the subsequent action of β-glucosidases (Chávez-Guerrero et al., 2019).

Xylanase is another enzyme with hydrolytic action that is effective in isolating nanocellulose. From the removal of xylan, this enzyme promotes the partial degradation of hemicelluloses into oligosaccharides (Hassan et al., 2010). Furthermore, like cellulases, xylanase hydrolyses terminal regions of cellulose fibers, breaking the β-(1,4)-glycosidic bonds of glucose units (Pääkko et al., 2007). Finally, the full action of xylanase can result in increased α-cellulose content and the degree of polymerization of cellulose (Hassan et al., 2010).

Salicornia ramosissima is a halophyte plant found in coastal areas worldwide, and in recent years started being industrially produced in Portugal in greenhouses for human consumption mainly in Mediterranean gourmet cuisine (Lima et al., 2020). Its production in greenhouses generates residues such as lower parts, namely stems and roots, which are discarded as they have no commercial value. The use of this biowaste for the use of cellulose can make salicornia production sustainable, contributing to the reduction of organic waste deposition in the environment and generating new income for the industry. The Salicornia waste is composed essentially of stems and roots and recent studies have explored its antioxidant potential (Pinto et al., 2021), whereas no studies are reporting its potential as a source of cellulosic fiber nor on the success of an enzyme treatment to isolate the nanofibers from this raw material.

This study aimed to investigate the potential of two nanofibers isolation processes, the conventional treatment by acid hydrolysis and a proposed method by enzymatic hydrolysis, and to compare the isolated CNFs for further use as a potential reinforcement agent.

2. Materials and methods

2.1. Waste recovery

The waste streams of the agro-industrial production of *Salicornia ramosissima*, namely stems and roots, were collected at Ria Fresh, an Algarve venture producing halophyte plants for human consumption using a soilless system. This production system and the characteristics of the plant, allow the same plant to produce *S. ramosissima*, with the ideal characteristics for consumption between 3 and 4 cuts. Thus, after this stage, the entire lower part of the plant was discarded and collected.

After collection in the greenhouse, the whole waste was transported to the food processing laboratory (DEA-UAlg), where they were cleaned and washed in flowing water to remove excess soil, and then stored frozen in a freezer at – 20 °C, until further processing.

2.2. Processing and powder preparation

Following collection, cleaning, and washing, the samples were dried in an industrial oven (Cassel, Germany) for 48 h at 50 °C, presenting in the end of this procedure a residual humidity of 5.2 ± 0.5%. Then, the dried waste was ground in an industrial mill (Retsch GmbH - Model: SM1, Germany) to obtain the bran. After grinding, the entire bran was sieved in a magnetic sieve shaker (Retsch GmbH, Germany) for the separation and measurement of microparticles (granulometry). As a result, the material sieved through the 140-mesh sieve afforded microparticles ≤ 110 μm that were used in the subsequent experiments. After processing, the bran of salicornia waste was weighed to determine the percentage of water loss during the drying process.

2.3. Production of CNFs

As part of the cellulose extraction, non-cellulosic components were removed according to Ventura-Cruz and Tecante (2019), but with a few modifications. By ethanol extraction (1:15 w/v) at 70 °C for 4 h under constant stirring, extractives (e.g., lipid fraction, phenolics, and pigments) were first removed. Then, the mixture was cooled to room temperature and filtered by vacuum filtration with a coarse pore filter. The insoluble fraction was dried in an oven at 50 °C for 24 h, obtaining a dark brown powder. Subsequently, other non-cellulosic components such as hemicelluloses, lignins, and pectins were removed by alkaline treatment, where the dry sample was mixed with sodium hydroxide (NaOH) 15% (1:15 w/v) and then with hydrogen peroxide 30% (H_2O_2) (100:1.2 v/v) and hydrolyzed under constant stirring at 50 °C for 3 h. The insoluble fraction was again separated by vacuum filtration with a coarse pore filter and washed with distilled water until the removal of dark liquor and obtaining a neutral pH.

Lastly, the sample was bleached to break down the phenolic compounds as well as to remove the by-products of this degradation. A mixture of NaOH (5%) and H_2O_2 (30%) at a ratio of 2:1 (v/v) was used to bleach the insoluble residue (ratio of 1:10 w/v) at 60 °C for 1 h under constant stirring. To avoid the foaming reaction a solution of acetic acid (10%) was used to neutralize the mixture. To achieve the ideal whitening of the pulp, a second bleaching process was performed under similar conditions as the first.

2.3.1. CNFs isolation by acid hydrolysis

Following the procedure described by Pelissari et al. (2014) with some modifications, mild acid hydrolysis was used to hydrolyze amorphous cellulose, remove mineral traces, and obtain nanofibers. The bleached sample was mixed with 2% sulphuric acid (H_2SO_4) (ratio of 1:20 w/v) at 80 °C for 2 h under constant agitation. Then the hydrolysate was centrifuged (centrifuge 3K20, Sigma Aldrich, GmbH-Germany) at 6000 rpm for 20 min, and the supernatant was neutralized with NaOH (40%). After successive centrifugations at 6000 rpm for 10 min to remove the sodium sulfate produced during neutralization, the solid fraction was washed with deionized water. Then, it was homogenized (T25 Digital ultra-turrax IKA, USA) at 13000 rpm for 5 min. The suspension was then filtered in coarse and fine pore paper (Whatman®, UK), and lyophilized (LyoQuest HT40, Telstar, Spain).

2.3.2. Proposed enzymatic process

The proposed enzymatic hydrolysis was performed by mixing the wet biomass with potassium phosphate buffer 0.08 M, pH 6 ± 0.1 (ratio of 1:10 w/v). A solution of hydrochloric acid (HCl) 0.325 N was used to correct the pH 6 of the mixture. Then, was added 30 μL of xylanase (endo-1,4-β-Xylanase, Megazyme) from *Trichoderma longibrachiatum* (1600 U/mL) in 3.2 M ammonium sulfate. After 60 min in a thermostatic bath (OVAN, BS127E, Spain) with horizontal shaking, the mixture was immediately cooled under constant stirring (100 rpm) in an ice bath until room temperature

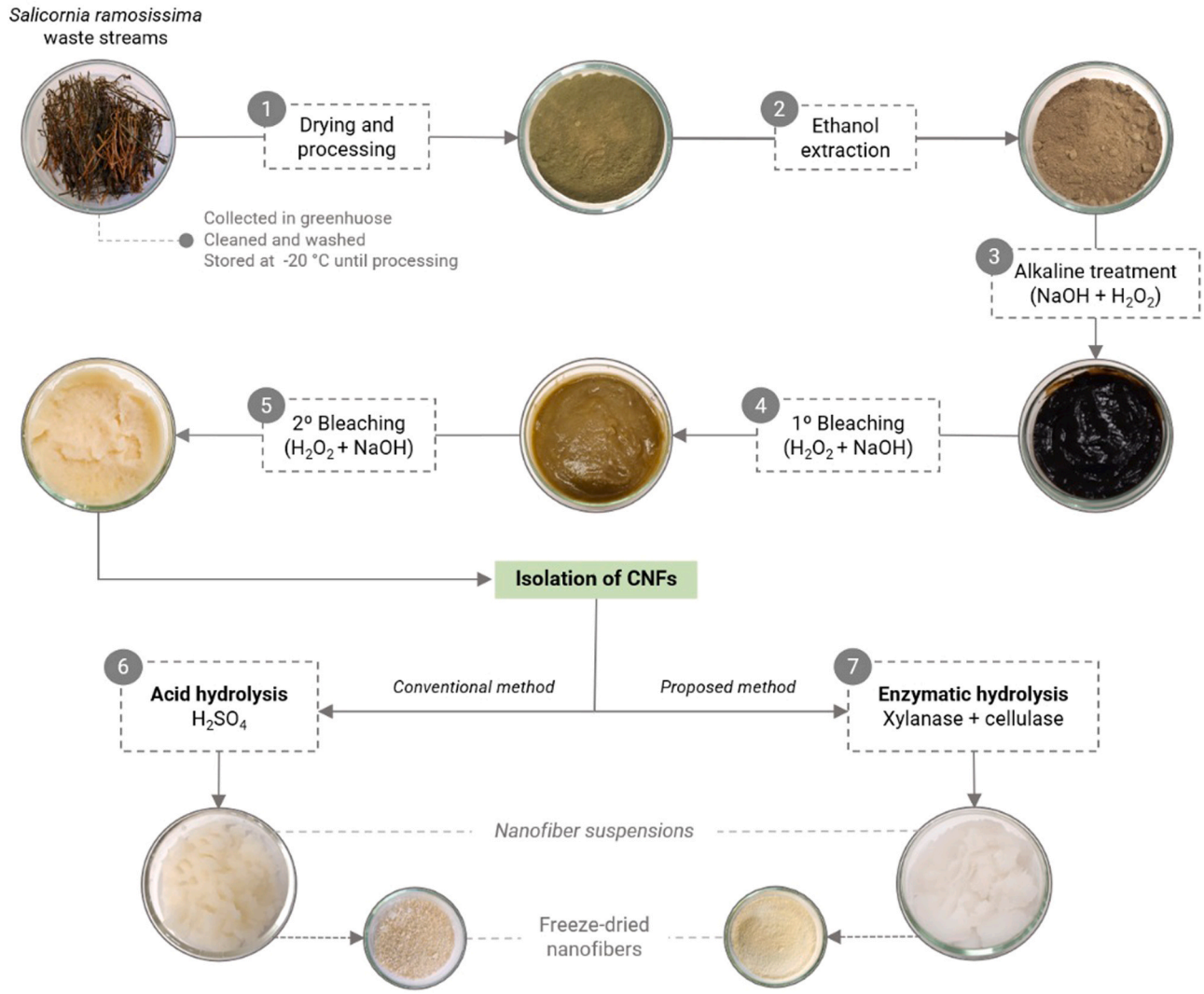

Fig. 1 – Flowchart of the process of CNFs production.

was reached. In the second part, the pH of the mixture was adjusted to 4.5 ± 0.1 with 0.325 N HCl and was added 15 µL of cellulase (endo-cellulase, Megazyme) from *T. longibrachiatum* (700 U/mL) in 3.2 M ammonium sulfate. Once again, the mixture was placed in a thermostatic bath under the same temperature, stirring, and time conditions as previously. Lastly, the mixture was allowed to remain in the thermostatic bath for 10 min at 100 °C to stop the enzymatic activity and then it was cooled in an ice bath until room temperature, vacuum filtered with fine pore filter paper, washed with 100 mL of deionized water, and stored at – 20 °C until lyophilization. An overview of the production of CNFs can be found in Fig. 1, from residue acquisition to nanocellulose isolation.

2.4. Characterization

2.4.1. Chemical composition of waste

After processing the salicornia waste, the powder was characterized chemically according to the following procedures: Ash (AOAC, 2016), total extractives content (Sluiter et al., 2008), cellulose content (Sun et al., 2004), and lignin content (Sluiter et al., 2012). The calculations for total extractives, ash, cellulose, lignin, and polysaccharides content including hemicellulose are shown below (eq.s 1–6).

Total extractives content (*TE*):

$$\%TE = \frac{(W_{bf} - W_{bo})}{W_s} * 100 \quad (1)$$

where, W_s is the initial sample weight (g); W_{bo}, is the empty flask´s initial weight (g); and W_{bf}, is the final weight of the flask with the extracted sample (g).

Cellulose content (*C*):

$$\%C = \frac{(W_{p+s} - W_{ed})}{W_{s(ef)}} * 100 \quad (2)$$

where, W_{p+s}, is the petri dish weight + final sample weight (g); W_{ed}, is the empty and tared dish weight (g); and $W_{s(ef)}$, is the initial sample weight (extractives free) (g).

Isoluble lignin ($L_{insoluble}$):

$$\%L_{insoluble} = \frac{(W_{p+s} - W_{ash})}{W_{s(ef)}} * 100 \quad (3)$$

where, W_{p+s}, is the petri dish weight + final sample weight (g); W_{ash}, is the ash weight (g); and $W_{s(ef)}$, is the initial sample weight (extractives free) (g).

Soluble lignin ($L_{soluble}$):

$$\%L_{soluble} = \frac{(ABS * V_f * F_d)}{(\varepsilon * W_{s(ef)})} * 100 \quad (4)$$

where, *ABS* is the absorbance at 240 nm; V_f, is the filtrate volume; F_d, is the dilution factor = 1; Ɛ, is the absorption constant for biomass versus wavelength = 198; and $W_{s(ef)}$, is the initial sample weight (extractives free) (g).

The amount of total lignin (*TL*) was calculated according to Eq. (5):

$$\%TL = \%L_{insoluble} + \%L_{soluble} \quad (5)$$

Percentage of polysaccharides including hemicellulose (*H*):

$$\%H = 100 - (\%TE + \%Ash + \%C + \%TL) \quad (6)$$

2.4.2. *Concentration of nanofibers suspension*

The procedure to concentrate the nanofiber suspensions followed the method described by Tibolla et al. (2014) by drying the suspensions in an oven at 105 °C for 24 h. The result was obtained by calculating the difference in mass of the sample before and after drying.

2.4.3. *Scanning electron microscopy (SEM)*

The microstructure of the powder waste, as well as the CNFs obtained by both methods, were analyzed by scanning electron microscopy (SEM) (Hitachi, model S-2400, Japan) equipped with an X-ray energy dispersion spectrometry microanalysis system (EDS) (Bruker, USA). The samples were prepared for observation by covering with gold/palladium (Au/Pd), in a sputter coater (Quorum Technologies, model Q150TES). Micrographs of the prepared aliquots were taken at an acceleration voltage of 20 kV.

2.4.4. *Transmission electron microscopy (TEM)*

To evaluate the efficiency of the methods used to obtain the CNFs and the structural and morphological characteristics, both the powder waste and the CNFs were evaluated using a transmission electron microscope (TEM) (Hitachi, model H8100, Japan), with a LaB6 filament operated at 200 kV. Digital images were acquired with a bottom-mounted CCD Keen-View camera (Olympus Soft Imaging Solutions GmbH, Germany). The average length of both the salicornia waste streams (SWS) and CNFs, was measured through the image processing analysis software ImageJ (NIH, USA).

2.4.5. *Dynamic light scattering (DLS) measurements*

The nanofibers were characterized by measuring their length, and surface charge (ζ-potential) using a DLS apparatus (Zetasizer Nano ZS, Malvern Instruments Ltd., UK). Measurements were performed in triplicate, at 25 °C, where 40 µL of each aqueous suspension were mixed with 1 mL of Milli-Q water and introduced into an electrophoretic cell (Malvern, Folded Capillary Zeta Cell - model DTS1070, UK) and analyzed by photon correlation spectroscopy and laser Doppler anemometry, respectively.

2.4.6. *X-ray diffraction (XRD)*

Powder X-ray diffractograms were recorded on an X-ray Diffractometer (Malvern, PANalytical X′Pert Pro powder, Malvern Instruments Ltd., UK), operating at 45 kV and 35 mA. The patterns of the raw material and samples of CNFs were recorded in the range 10–80° (2θ) with a step size of 0.0167° and 100 s per step using nickel-filtered CuKα radiation with a wavelength of 0.154 nm using an X′Celerator detector. The crystallinity index (*CrI* %) of the samples was calculated using Eq. (7), according to the procedure reported by Segal et al. (1959).

$$CrI = \frac{(I_{002} - I_{am})}{I_{002}} * 100 \quad (7)$$

where, I_{002} = is the maximum intensity (in arbitrary units) close to 2θ = 22–24°, which refers a crystalline material, and I_{am} is the intensity of diffraction in the same units at 2θ = 18°, which refers to amorphous material in cellulosic fibers. All data were processed using the OriginPro 2021b graphic software (OriginLab Corporation, USA).

2.4.7. *Fourier Transform Infrared Spectroscopy (FTIR)*

FTIR tests were performed to the analysis of the functional groups present in the powder of *S. ramosissima* waste and the CNFs. The samples were previously grounded with KBr in a mortar and compressed into discs. FTIR spectra were recorded in an FT-IR spectrophotometer (Bruker, model Tensor 27, USA) For each spectrum, a 32-scan interferogram was collected in transmittance mode with a 4 cm^{-1} resolution in the 4000–400 cm^{-1} region, and the results were obtained using the eFTIR software (Essential FTIR®, USA).

2.5. *Statistical analysis*

Results were expressed as mean ± standard error of the mean, and experiments were conducted at least in triplicate. Significant differences were assessed by analysis of variance (ANOVA) using the Tukey HSD (honestly significant differences) test. Statistical analysis was performed using Statistica 7.0 software (Statsoft Inc., USA).

3. Results and discussion

3.1. *Chemical composition*

The chemical composition of *S. ramosissima* waste (stems and roots) is presented in Table 2. Being a waste that comes from a non-conventional raw material, but promising from the point of view of production, marketing, and consumption, it is relevant to compare these results with other cellulosic wastes and by-products successfully used to isolate cellulose and nanocellulose.

The cellulose content of *S. ramosissima* waste is comparable to the content of other agricultural wastes, such as cassava pomace, apple, and tomato pomace. In this sense, the use of this waste can be a promising bet with good added value prospects.

After drying, the *S. ramosissima* waste (as obtained from industry), a water loss of 68.3% was observed.

3.2. *Appearance, CNF suspensions concentration and yield*

Fig. 1 shows all the steps for isolating CNFs from *S. ramosissima* waste streams. After drying and milling (step 1), the waste in powder with an intense green color was submitted to ethanol extraction (step 2) to remove the lipid fraction and phenolic substances (Malucelli et al., 2017), changing its color to light brown. Then the sample was treated with an alkaline solution (step 3) for hydrolysis of components such as starch, hemicellulose, lignin, and pectins, converting the initial light brown color into a dark brown color. These changes may be associated with fast-chain degradations,

Table 2 – Chemical composition of the salicornia waste compared to other agro-industrial waste.

Agro-industrial waste	Total extractives (%)	Ash (%)	Cellulose (%)	Lignin (%)	Polysaccharides (%)[a]	Reference
Salicornia waste	13.5 ± 0.5	0.33 ± 0.1	17.6 ± 0.6	13.1 ± 0.8	55.6 ± 1.0	
Apple pomace	17.8	–	8.81	2.98	–	(Szymańska-Chargot et al., 2017)
Banana peels	9.60	0.01	7.5	7.9	74.9	(Tibolla et al., 2014)
Carrot pomace	13.1	–	10.0	2.50	–	(Szymańska-Chargot et al., 2017)
Cassava bagasse	–	–	6.70	2.01	89.9	(Leite et al., 2017)
Cassava peelings	–	–	14.8	12.8	50.3	(Leite et al., 2017)
Cucumber pomace	5.57	–	16.1	4.51	–	(Szymańska-Chargot et al., 2017)
Grape pomace	–	3.58	19.3	15.7	–	(Coelho et al., 2018)
Tomato pomace	6.03	–	8.60	5.85	–	(Szymańska-Chargot et al., 2017)

[a] Polysaccharides including hemicellulose

alkali-induced condensation promoted by beta-elimination reactions of carbonyl groups, and potentiated not only by the alkaline media with a high pH but also by the temperature (Ahn et al., 2019). Bleaching (steps 4 and 5) was conducted in two sequential steps and proved to be efficient in removing the components responsible for the brown color of the solid fraction, such as lignin and tannins. According to (Dufresne et al. (1997) in bleaching, chlorine and chlorites promote rapid oxidation of lignin, generating carbonyl, carboxylic and hydroxyl groups, solubilizing the lignin, removing the hemicellulose, and purifying the cellulose. The result is consistent with Pelissari et al. (2014) and Ventura-Cruz & Tecante (2019) who also used chemical treatment followed by bleaching to solubilize hemicellulose and delignify the cellulose in banana peels and Rose stems, respectively. After two bleaching steps, the solid fraction (cellulose) developed a light yellowish color, tending to white. The low capacity of the alkaline treatment to remove the lignin may be one of the answers to the poor performance of bleaching to solubilize hemicellulose and hydrolyze the cellulose chains. According to Tibolla et al. (2014), in a study with banana peels the remaining lignin may have developed a barrier around the cellulose and hemicellulose, preventing the reactions in the bleaching step to occur. Next, the solid fraction was split into two equal parts to different hydrolysis processes (step 6).

The acid hydrolysis was ineffective at removing the remaining lignin fractions, resulting in the same light-yellow coloration. As for the enzymatic hydrolysis (proposed method), it proved to be effective at removing the light-yellow coloration resulting in a white nanocellulose, with a high purity level, suggesting that the amorphous components were completely removed. The success of this method can be attributed to the enzyme's ability to attack the amorphous regions of lignocellulosic fibers, through which their larger contact area and lower density allow hydrolytic cleavage of the β-1,4 glycosidic bonds that connect the glucose units into cellulose.

Cellulase is an enzymatic complex formed by three enzymes that act in synergism (endoglucanase, exoglucanase, and β-glucosidase), and it can degrade cellulose into sugar monomers. However, to isolate CNFs, a cellulase composed only of endoglucanase has ideal properties to initiate hydrolysis specifically at the ends of the cellulose chain (Chávez-Guerrero et al., 2019; Pääkko et al., 2007). On another hand, xylanase is a hydrolytic enzyme that randomly catalyzes the hemicellulose compounds present in the vegetable fiber. In this study, the enzymatic hydrolysis started with the action of cellulase on the cellulose chains followed by the selective hydrolysis of xylanase on the fibrils promoting the formation of CNFs.

The concentration of nanofibers in the suspension (g of nanofibers / 100 g of suspension) obtained by AT and ET was 6.2 ± 0.2 and 7.3 ± 0.1, respectively. As a result, the yield for CNF (AT) and CNF (ET) was 4.8 ± 0.3% and 5.5 ± 0.2%, respectively, when calculating the weight difference between the amount of SWS before ethanol extraction and the amount of CNFs after lyophilization. This yield is close to the 5.1% obtained by (Tibolla et al. (2014) for banana peels nanofibers obtained by a chemical process. In this context, the low yield values can be attributed to the several stages during the AT and ET, with a wide optimization margin considering the transition from the laboratory to the pilot scale.

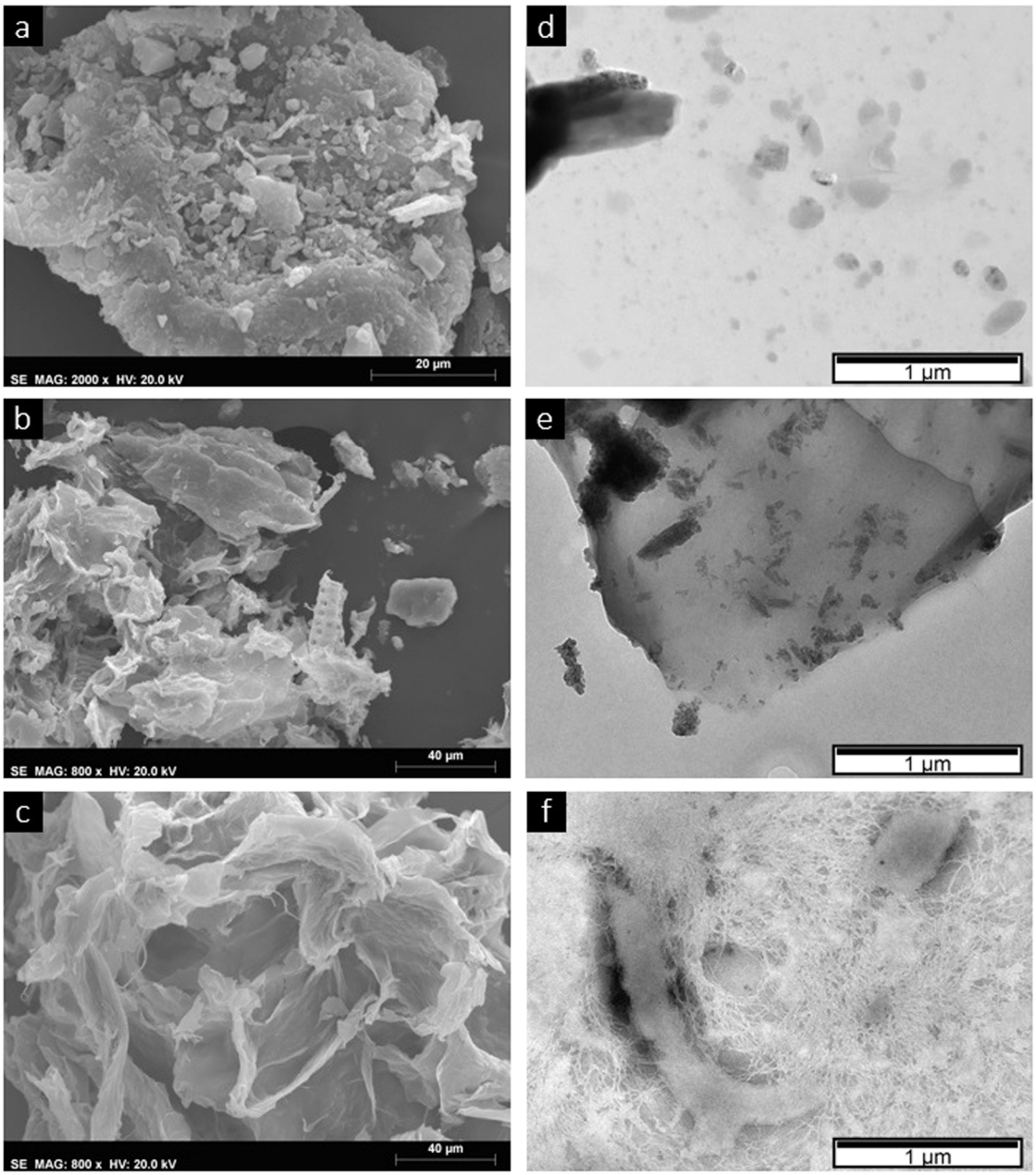

Fig. 2 – SEM micrographs of SWS (a), CNFs by acid (b) and enzymatic (c) treatment, and TEM images of SWS (d), CNFs by acid (e), and enzymatic (f) treatment.

3.3. *SEM and TEM analysis*

SEM micrographs of the SWS and CNFs (Fig. 2a, b, c) provided a view of the structure of the crude fiber and the morphological changes in the fibers promoted by treatments (chemical and enzymatic) to obtain the nanofibers. The SWS had an irregular surface with residues of different sizes because of the processing step. In the CNFs, the gradual removal of amorphous components (hemicellulose and lignin) and the permanence of the cellulosic portion were evident, mainly in the CNF (ET). These results corroborate those of other authors who also observed morphological changes in fibers from different residues and by-products of plant matrix, applying different chemical and enzymatic treatments for nanocellulose obtention. As in the CNFs from olive tree pruning (Sánchez-Gutiérrez et al., 2021), CNFs from rose stems (Ventura-Cruz and Tecante, 2019), cellulose nanocrystals (CNCs) from sugar palm fibers (Ilyas et al., 2018), and CNFs cassava root pomace and peelings (Leite et al., 2017).

The analysis of the visual aspect of the TEM images (Fig. 2d, e, f) showed that AT and ET isolated the CNFs. Overall, the enzymatic treatment was more effective in removing minerals traces and hydrolyzing the amorphous cellulose. This result can be related to the weak acid treatment, H_2SO4 (2%). However, the TEM images show traces of components such as hemicelluloses and lignin as well as the formation of interfibrillar hydrogen bonds in both CNFs, evidencing the need for optimization in the removal and hydrolysis steps, or even the addition of mechanical treatment (high-pressure homogenizer). According to Pelissari et al. (2014), the addition of a mechanical treatment increased the removal process of the undesirable components and improved the properties of nanofibers from banana peels subjected to acid treatment, H_2SO_4 (1%).

Table 3 – Characterization of CNFs obtained by acid and enzymatic treatment.

Sample	Diameter, D (nm)	Length, L (nm)	Aspect ratio, (L/D)	Polidispersity index, PdI	ζ-potencial (mV)
AT	17.9 ± 2.8[a]	928.6 ± 38.5[a]	51.7 ± 2.1[a]	0.77 ± 0.04[a]	-42.5 ± 2.1[a]
ET	13.5 ± 0.9[b]	984.0 ± 30.9[a]	72.7 ± 2.3[b]	0.79 ± 0.03[a]	-52.2 ± 3.7[b]

Different letters indicate significant differences between samples ($p < 0.05$).

The diameters of the CNFs (AT) and (ET) were 17.9 and 13.5 nm, respectively. This result confirmed the effectiveness of both processes in isolating the fibers from the *S. ramosissima* residue on a nanometric scale. According to Espinosa et al. (2017), the sizes of nanofibers can vary between different raw materials even when applying similar production processes. Furthermore, according to Leite et al. (2017), the hydrolysis time and the acid concentration are also variables that influence the final size of the nanofibers.

In this study, the sizes of the CNFs are close to those of nanometric structures extracted from other agro-residue sources chemically or enzymatically treated, such as CNFs from cassava pomace (15–30 nm) (Panyasiri et al., 2018), CNCs from sugar palm fibers (3 –18.2 nm) (Ilyas et al., 2018), CNCs from grape pomace (3–10 nm) (Coelho et al., 2018), and CNFs from banana peels (7.6–22.6 nm) (Pelissari et al., 2014; Tibolla et al., 2014).

3.4. *Particle size distribution and ζ-potential*

Table 3 presents a characterization of nanofibers based on their particle diameter (D), length (L), and aspect ratio (L/D). As a general trend, the enzymatic treatment obtained smaller diameter nanofibers, but the difference in length was not significant ($p < 0.05$). On the other hand, the aspect ratio of CNF (ET) was significantly higher, 72.7, while for CNF (AT), it was 51.7. Despite the differences between nanofibers, the high aspect ratio (between 50 and 300) shows that both results were good enough to show that CNFs have great applicability in materials science, whether to produce robust aerogels (Kettunen et al., 2011; Wang et al., 2018) or to be used as reinforcing agents in polymeric compositions (Norrrahim et al., 2021). Several studies have related the highest aspect ratio of continuous fibers with a high degree of entanglement, resulting in nanofibers with greater efficiency in general mechanical properties such as stiffness, flexural strength, elasticity modulus, and traction (Li et al., 2014; Malyshev et al., 2021; Norrrahim et al., 2021; Zárate et al., 2003).

Fig. 3 shows the granulometric distribution represented as a volume percent. Peaks reveal a modal distribution of the samples, with only one distribution peak. According to Leite et al. (2017), the volumetric distribution weighs larger particles more heavily because the particles' volume is a cubic function of the diameter, not taking smaller particles into account. For SWS, most particles were in the equivalent volume diameter range of 419–951 nm. For CNFs, the range of equivalent diameter related to the volumetric distribution was smaller, between 230 and 756 nm for CNF(AT) and 151–525 nm for CNF(ET). Overall, the distribution of CNF (ET) was lower than that of CNF (AT), and according to Tibolla et al. (2014), this behavior indicates that the enzymatic treatment was more severe, showing a greater capacity for destruction of crystalline zones and greater degradability of amorphous zones of fibers.

The effect of the acid and enzymatic treatments on the zeta potential is present in Table 3. The zeta potential was – 42.5 ± 2.1 for the CNF (AT) and – 52.2 ± 3.7 mV for CNF (ET). The first relevant observation is that both nanofibers have a negative charge. The higher negative charges of CNF (ET) indicate characteristics of a nanofiber with good electrical stability, therefore, with better performance as a reinforcing agent. Jiang and Hsieh (2015) reported that the hydrolysis of sulfuric acid promoted the stabilization of the aqueous suspension of nanocellulose by negatively charged sulfate groups, confirmed with a zeta potential of – 52.4 mV, similar to the zeta potential of CNF (ET). Tibolla et al. (2014) observed that the enzymatic treatment with xylanase resulted in nanofibers with high electrostatic repulsion and less capacity for aggregation between fibers. In this sense, as in the present study, the nanofibers obtained by enzymatic treatment showed an ability to form more effective surface charges to stabilize the suspension instead of the nanofibers obtained by the acid treatment.

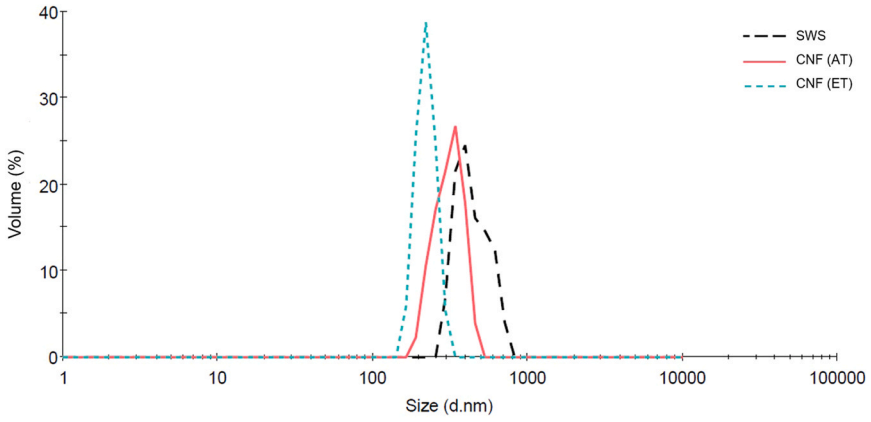

Fig. 3 – Particle size volumetric distribution of SWS and CNFs.

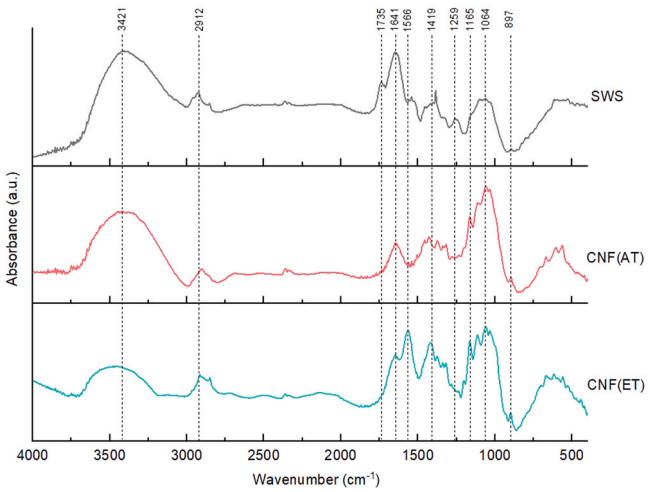

Fig. 4 – FTIR spectra of SWS and CNFs obtained by acid and enzymatic treatment.

3.5. *FTIR spectroscopy analysis*

The spectra of SWS and CNFs (AT) and (ET) are shown in Fig. 4. All spectra showed peaks in the region of 3421 cm^{-1} which are a characteristic of the –OH elongation vibrations, in cellulose, typical of hydrogen bonding molecules (Ilyas et al., 2018; Sánchez-Gutiérrez et al., 2020).

The peak found in the 2912 cm^{-1} region occurred due to the existence of alkane groups in the cellulose chain. Overall, peaks around the region between 2950 and 2850 cm^{-1} are characteristic of C–H asymmetric elongation vibrations (Pelissari et al., 2014; Roy et al., 2021). The peak showed at 1735 cm^{-1}, present only in the SWS sample, represents vibrations of the acetyl and uronic ester groups of hemicelluloses or to the ester linkage of the carboxylic group of the ferulic and *p*-coumaric acids of lignin (Cherian et al., 2008). According to Tibolla et al. (2018), the absence of this peak in the CNFs spectra is due to the process of complete or partial removal of hemicelluloses and lignin through bleaching. The absorption bands observed at 1641 and 1566 cm^{-1} can be associated with adsorbed water and elongation of aromatic lignin groups (Ilyas et al., 2018; Ventura-Cruz and Tecante, 2019). For this reason, some of these peaks may have been low intensity in the CNFs where lignin was previously present. The peak at 1419 cm^{-1} is attributed to the elongation of the C–H groups and the curvature mode of the CH_2 bonds (Sánchez-Gutiérrez et al., 2020). Small absorbance bands observed between 1500 and 1100 cm^{-1} were attributed to proteins (Jiang and Hsieh, 2015).

In general, peaks that emerge below 1300 cm^{-1} are in a region known as the cellulose fingerprint zone (Kafle et al., 2015). The absorbance bands around 1259, 1161, and 1064 cm^{-1} represent asymmetric CO–O–C elongations of esters and glycogen and the C–H curvature in aromatic rings. Probably, in CNFs, the peak is associated with changes in hydrogen bonds, suggesting a transition from cellulose I to cellulose II (Leite et al., 2017; Sun et al., 2004). The observed absorbance band at 897 cm^{-1} is attributed to C–H vibrations associated with *b*-glycosidic bonds between glucose units in cellulose molecules (Hassan et al., 2010).

The likely functional groups of the biochemical compounds present in the samples, based on similar biological systems described in the literature, are summarized in Table 4.

3.6. *XRD patterns*

Fig. 5 shows the XRD patterns of the *S. ramosissima* waste and the CNFs obtained by AT and ET. The fibers from the untreated salicornia waste (SWS) showed a large amorphous portion mainly by the presence of hemicellulose and lignin. On the other hand, the CNFs obtained by AT and ET presented a larger crystalline region with partially similar XRD patterns occurring at 2θ angles of 16, 22, 32, and 34 degrees. All these crystallographic planes are typical of the presence of cellulose I, or pure cellulose (Naduparambath et al., 2018; Ventura-Cruz and Tecante, 2019; Xing et al., 2020). Moreover, the CNF diffractograms showed high intensity and well-shaped peaks, indicating structural changes in the fibers, a characteristic of crystalline samples with high cellulose quantity and low or no presence of hemicelluloses and lignin fractions (Jiang and Hsieh, 2015; Mussatto et al., 2008).

The crystallinity index of the CNFs doubled that of the SWS fibers. While SWS fibers presented *CrI* of 25.4%, the CNFs obtained by AT and ET presented indexes of 61.8% and 63.8%, respectively. In this context, the acid and enzymatic treatments promoted the isolation process of CNFs through the purification and realignment of cellulose molecules also the increasing the crystalline surface (Jonoobi et al., 2015; Leite et al., 2017). Several studies with raw materials and by-products of vegetable origin reported the increase in the crystallinity degree after acid or enzymatic hydrolysis, with similar results to those obtained in this study. Other authors proposed the isolation of nanocellulose from other plant by-products and found an increase in *CrI*, as in nanocellulose obtained from soy hulls, 64.4% (Flauzino Neto et al., 2013), banana peels, 58.6% (Tibolla et al., 2014), Rose stems, 56.2% (Ventura-Cruz and Tecante, 2019), grape pomace, 74.9% (Coelho et al., 2018), olive tree harvest, 48.9% (Sánchez-Gutiérrez et al., 2020). Both the acid and the enzymatic treatment were successfully used in the previous examples, under varying conditions of concentration of enzyme, acid solution, temperature, and time.

The advantage of the crystallinity index of CNFs obtained by the proposed enzymatic treatment (63.8%) compared to the CNFs obtained by acid treatment (61.8%) may be related to the lack of optimization of the acid hydrolysis process. Liu et al. (2016) observed that during the acid hydrolysis, the time and acid concentration hydrolyze the amorphous regions of

Table 4 – Summary of FTIR spectral analysis.

Wavenumber (cm^{-1})	Functional groups and vibrational modes	Biochemical compounds	Samples			References
			SWS	CNF (AT)	CNF (ET)	
3390–3431	–OH stretching	Water	✓	✓	✓	Ilyas et al., 2018; Sánchez-Gutiérrez et al., 2020
2925–2901	CH_2, CH_3 asymmetric stretching	Hemicellulose and cellulose	✓	✓	✓	Pelissari et al., 2014; Roy et al., 2021
1734	C_2H_3O and CH_2OH groups vibration	Hemicellulose	✓	×	×	Cherian et al., 2008;Tibolla et al., 2018
1641–1566	Adsorbed H_2O and C=O vibrations	Lignin	✓	✓	✓	Ilyas et al., 2018; Ventura-cruz and Tecante, 2019
1430–1311	C-H group stretching;	Lignin	✓	✓	✓	Sánchez-Gutiérrez et al., 2020;Tibolla et al., 2014
1180–1058	CO–O–C asymmetric stretching	Cellulose I and Cellulose II	✓	✓	✓	Leite et al., 2017;Sun et al., 2004
897	C-H vibration	Cellulose	×	✓	✓	Hassan et al., 2010

✓: present; ×: absent.

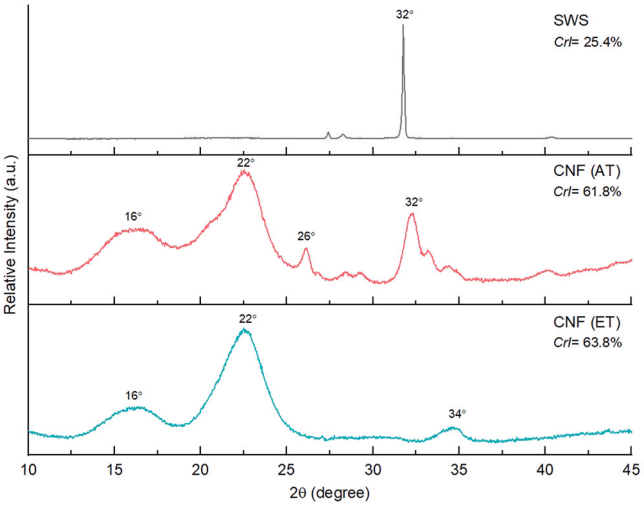

Fig. 5 – XRD patterns and crystallinity index of SWS and CNFs, obtained by both methods.

cellulose, partially destroying, in the meantime, the crystallinity and reducing the potential of the process.

4. Conclusion

CNFs were successfully isolated by alkaline treatment, followed by bleaching and mild acid hydrolysis or enzymatic hydrolysis using the enzymes xylanase and cellulase (proposed method). The alkaline treatment and bleaching removed the amorphous portions with the removal of the hemicellulose and lignin, as shown in the FTIR studies. From SEM micrographs, it can be concluded that the enzymatic treatment was efficient in producing CNFs from plant waste. The TEM images showed that the nanofibers have a diameter in the range of 15.5–17.9 nm. Furthermore, nanofibers from AT e ET have a high aspect ratio (51.7 and 72.7), crystallinity index (61.8 e 63.8%), and ζ-potential (42.5 and –52.5 mV), respectively. XRD patterns of the extracted CNFs show typical cellulose I structures.

The proposed production scheme to obtain CNFs from the waste streams of the *S. ramosissima* can contribute to reducing costs with industrial waste management by successfully applying the circular economy concepts, in this case, when using a new kind of raw material to produce a product that already exists, the CNFs. Finally, it was proved that the residue of *S. ramosissima* can be used as a renewable source of nanofibers production. Furthermore, the enzymatic treatment can replace traditional methods without generating toxic residues, with mild thermal conditions, and produce nanocellulose with high-value applications in the material sciences.

Funding

This research was funded by National Funds through FCT - Foundation for Science and Technology, under the Project UIDB/05183/2020. Alexandre R. Lima and Nathana L. Cristofoli would like to acknowledge the FCT for awarding the doctoral research grants SFRH/BD/149398/2019 and SFRH/BD/149395/2019, respectively.

Declaration of Competing Interest

The authors declare that they have no known competing financial interests or personal relationships that could have appeared to influence the work reported in this paper.

Acknowledgments

The authors acknowledge Miguel Salazar and Carla Nunes from RiaFresh® (Faro, Portugal) for their support in this project, kindly providing the agro-industrial waste. Dr. João P. Lourenço for all his work and support at the X-Ray Diffraction, CIQA, University of Algarve. Furthermore, we would like to acknowledge Dr. Ana Grenha for the use of the Zetasizer equipment, CCMAR, at the University of Algarve.

References

Abdul Khalil, H.P.S., Davoudpour, Y., Islam, M.N., Mustapha, A., Sudesh, K., Dungani, R., Jawaid, M., 2014. Production and modification of nanofibrillated cellulose using various mechanical processes: a review. Carbohydr. Polym. 99, 649–665. https://doi.org/10.1016/j.carbpol.2013.08.069

Ahn, K., Zaccaron, S., Zwirchmayr, N.S., Hettegger, H., Hofinger, A., Bacher, M., Henniges, U., Hosoya, T., Potthast, A., Rosenau, T., 2019. Yellowing and brightness reversion of celluloses: CO or COOH, who is the culprit? Cellulose 26, 429–444. https://doi.org/10.1007/s10570-018-2200-x

Alcántara, J.C., González, I., Pareta, M.M., Vilaseca, F., 2020. Biocomposites from rice straw nanofibers: morphology, thermal and mechanical properties. Materials 13, 1–16. https://doi.org/10.3390/ma13092138

AOAC, 2016. Association of Official Analytical Chemists, 20th ed, The Official Methods of Analysis of AOAC International. AOAC International, Maryland, USA.

Ayala-Zavala, J.F., Vega-Vega, V., Rosas-Domínguez, C., Palafox-Carlos, H., Villa-Rodriguez, J.A., Siddiqui, M.W., Dávila-Aviña, J.E., González-Aguilar, G.A., 2011. Agro-industrial potential of exotic fruit byproducts as a source of food additives. Food Res. Int. 44, 1866–1874. https://doi.org/10.1016/j.foodres.2011.02.021

Ben-Othman, S., Jõudu, I., Bhat, R., 2020. Bioactives from agri-food wastes: present insights and future challenges. Molecules. https://doi.org/10.3390/molecules25030510

Chávez-Guerrero, L., Silva-Mendoza, J., Sepúlveda-Guzmán, S., Medina-Aguirre, N.A., Vazquez-Rodriguez, S., Cantú-Cárdenas, M.E., García-Gómez, N.A., 2019. Enzymatic hydrolysis of cellulose nanoplatelets as a source of sugars with the concomitant production of cellulose nanofibrils. Carbohydr. Polym. 210, 85–91. https://doi.org/10.1016/J.CARBPOL.2019.01.055

Cherian, B.M., Pothan, L.A., Nguyen-Chung, T., Mennig, G., Kottaisamy, M., Thomas, S., 2008. A novel method for the synthesis of cellulose nanofibril whiskers from banana fibers and characterization. J. Agric. Food Chem. 56, 5617–5627. https://doi.org/10.1021/jf8003674

Coelho, C.C.S., Michelin, M., Cerqueira, M.A., Gonçalves, C., Tonon, R.V., Pastrana, L.M., Freitas-Silva, O., Vicente, A.A., Cabral, L.M.C., Teixeira, J.A., 2018. Cellulose nanocrystals from grape pomace: production, properties and cytotoxicity assessment. Carbohydr. Polym. 192, 327–336. https://doi.org/10.1016/j.carbpol.2018.03.023

Dufresne, A., Cavaillé, J.Y., Vignon, M.R., 1997. Mechanical behavior of sheets prepared from sugar beet cellulose microfibrils. J. Appl. Polym. Sci. 64, 1185–1194 https://doi.org/10.1002/(sici)1097-4628(19970509)64:6<1185::aid-app19>3.3.co;2-2.

Espinosa, E., Sánchez, R., Otero, R., Domínguez-Robles, J., Rodríguez, A., 2017. A comparative study of the suitability of different cereal straws for lignocellulose nanofibers isolation. Int. J. Biol. Macromol. 103, 990–999. https://doi.org/10.1016/j.ijbiomac.2017.05.156

FAO, 2019. FAO. state food Agric. Mov. Forw. food loss waste reduction. 1–439. https://doi.org/10.4324/9781315764788.

Flauzino Neto, W.P., Silvério, H.A., Dantas, N.O., Pasquini, D., 2013. Extraction and characterization of cellulose nanocrystals from agro-industrial residue - Soy hulls. Ind. Crops Prod. 42, 480–488. https://doi.org/10.1016/j.indcrop.2012.06.041

Hansson, S., Östmark, E., Carlmark, A., Malmström, E., 2009. ARGET ATRP for versatile grafting of cellulose using various monomers. ACS Appl. Mater. Interfaces 1, 2651–2659. https://doi.org/10.1021/am900547g

Hassan, M.L., Mathew, A.P., Hassan, E.A., Oksman, K., 2010. Effect of pretreatment of bagasse pulp on properties of isolated nanofibers and nanopaper sheets. Wood Fiber Sci. 42, 362–376.

Henrissat, B., Bairoch, A., 1993. New families in the classification of glycosyl hydrolases based on amino acid sequence similarities. Biochem. J. 293, 781–788. https://doi.org/10.1042/bj2930781

Ilyas, R.A., Sapuan, S.M., Ishak, M.R., 2018. Isolation and characterization of nanocrystalline cellulose from sugar palm fibres (Arenga pinnata). Carbohydr. Polym. 181, 1038–1051. https://doi.org/10.1016/j.carbpol.2017.11.045

Jayasekara, S.and Ratnayake, R., 2019. Microbial Cellulases: An Overview and Applications, in: Pascual, A.R., Martín, M.E.E. (Eds.), Cellulose. IntechOpen, pp. 1–21. https://doi.org/10.5772/intechopen.84531.

Jiang, F., Hsieh, Y.Lo, 2015. Cellulose nanocrystal isolation from tomato peels and assembled nanofibers. Carbohydr. Polym. 122, 60–68. https://doi.org/10.1016/j.carbpol.2014.12.064

Jonoobi, M., Oladi, R., Davoudpour, Y., Oksman, K., Dufresne, A., Hamzeh, Y., Davoodi, R., 2015. Different preparation methods and properties of nanostructured cellulose from various natural resources and residues: a review. Cellulose 22, 935–969. https://doi.org/10.1007/s10570-015-0551-0

Kafle, K., Shin, H., Lee, C.M., Park, S., Kim, S.H., 2015. Progressive structural changes of Avicel, bleached softwood, and bacterial cellulose during enzymatic hydrolysis. Sci. Rep. 5, 1–10. https://doi.org/10.1038/srep15102

Kettunen, M., Silvennoinen, R.J., Houbenov, N., Nykänen, A., Ruokolainen, J., Sainio, J., Pore, V., Kemell, M., Ankerfors, M., Lindström, T., Ritala, M., Ras, R.H.A., Ikkala, O., 2011. Photoswitchable superabsorbency based on nanocellulose aerogels. Adv. Funct. Mater. 21, 510–517. https://doi.org/10.1002/adfm.201001431

Leite, A.L.M.P., Zanon, C.D., Menegalli, F.C., 2017. Isolation and characterization of cellulose nanofibers from cassava root bagasse and peelings. Carbohydr. Polym. 157, 962–970. https://doi.org/10.1016/j.carbpol.2016.10.048

Li, J., Song, Z., Li, D., Shang, S., Guo, Y., 2014. Cotton cellulose nanofiber-reinforced high density polyethylene composites prepared with two different pretreatment methods. Ind. Crops Prod. 59, 318–328. https://doi.org/10.1016/j.indcrop.2014.05.033

Lima, A.R., Castañeda-Loaiza, V., Salazar, M., Nunes, C., Quintas, C., Gama, F., Pestana, M., Correia, P.J., Santos, T., Varela, J., Barreira, L., 2020. Influence of cultivation salinity in the nutritional composition, antioxidant capacity and microbial quality of Salicornia ramosissima commercially produced in soilless systems. Food Chem. 333, 127525. https://doi.org/10.1016/j.foodchem.2020.127525

Liu, C., Li, B., Du, H., Lv, D., Zhang, Y., Yu, G., Mu, X., Peng, H., 2016. Properties of nanocellulose isolated from corncob residue using sulfuric acid, formic acid, oxidative and mechanical methods. Carbohydr. Polym. 151, 716–724. https://doi.org/10.1016/j.carbpol.2016.06.025

Madsen, B., Gamstedt, E.K., 2013. Wood versus plant fibers: Similarities and differences in composite applications. Adv. Mater. Sci. Eng. 2013. https://doi.org/10.1155/2013/564346

Malucelli, L.C., Lacerda, L.G., Dziedzic, M., da Silva Carvalho Filho, M.A., 2017. Preparation, properties and future perspectives of nanocrystals from agro-industrial residues: a review of recent research. Rev. Environ. Sci. Biotechnol. 16, 131–145. https://doi.org/10.1007/s11157-017-9423-4

Malyshev, M.D., Guseva, D.V., Vasilevskaya, V.V., 2021. Effect of Nanoparticles Surface Bonding and Aspect Ratio on Mechanical Properties of Highly Cross-Linked Epoxy Nanocomposites: Mesoscopic Simulations.

Marić, M., Grassino, A.N., Zhu, Z., Barba, F.J., Brnčić, M., Rimac Brnčić, S., 2018. An overview of the traditional and innovative approaches for pectin extraction from plant food wastes and by-products: Ultrasound-, microwaves-, and enzyme-assisted extraction. Trends Food Sci. Technol. 76, 28–37. https://doi.org/10.1016/j.tifs.2018.03.022

Mussatto, S.I., Fernandes, M., Milagres, A.M.F., Roberto, I.C., 2008. Effect of hemicellulose and lignin on enzymatic hydrolysis of

cellulose from brewer's spent grain. Enzym. Microb. Technol. 43, 124–129. https://doi.org/10.1016/j.enzmictec.2007.11.006
Müssig, J., 2010. Industrial applications of natural fibres: structure, properties and technical applications. Ind. Appl. Nat. Fibres Struct. Prop. Tech. Appl. 538. https://doi.org/10.1002/9780470660324
Naduparambath, S., T.V, J., Shaniba, V., M.P, S., Balan, A.K., Purushothaman, E., 2018. Isolation and characterisation of cellulose nanocrystals from sago seed shells. Carbohydr. Polym. 180, 13–20. https://doi.org/10.1016/j.carbpol.2017.09.088
Norrrahim, M.N.F., Kasim, N.A.M., Knight, V.F., Halim, N.A., Shah, N.A.A., Noor, S.A.M., Jamal, S.H., Ong, K.K., Wan Yunus, W.M.Z., Farid, M.A.A., Jenol, M.A., Ahmad, I.R., 2021. Performance evaluation of cellulose nanofiber reinforced polymer composites. Funct. Compos. Struct. 3. https://doi.org/10.1088/2631-6331/abeef6
Pääkko, M., Ankerfors, M., Kosonen, H., Nykänen, A., Ahola, S., Österberg, M., Ruokolainen, J., Laine, J., Larsson, P.T., Ikkala, O., Lindström, T., 2007. Enzymatic hydrolysis combined with mechanical shearing and high-pressure homogenization for nanoscale cellulose fibrils and strong gels. Biomacromolecules 8, 1934–1941. https://doi.org/10.1021/bm061215p
Panyasiri, P., Yingkamhaeng, N., Lam, N.T., Sukyai, P., 2018. Extraction of cellulose nanofibrils from amylase-treated cassava bagasse using high-pressure homogenization. Cellulose 25, 1757–1768. https://doi.org/10.1007/s10570-018-1686-6
Pelissari, F.M., Sobral, P.J.D.A., Menegalli, F.C., 2014. Isolation and characterization of cellulose nanofibers from banana peels. Cellulose 21, 417–432. https://doi.org/10.1007/s10570-013-0138-6
Pinto, D., Reis, J., Silva, A.M., Salazar, M., Dall'Acqua, S., Delerue-Matos, C., Rodrigues, F., 2021. Valorisation of Salicornia ramosissima biowaste by a green approach – An optimizing study using response surface methodology. Sustain. Chem. Pharm. 24, 100548. https://doi.org/10.1016/j.scp.2021.100548
Ribeiro, R.S.A., Pohlmann, B.C., Calado, V., Bojorge, N., Pereira, N., 2019. Production of nanocellulose by enzymatic hydrolysis: trends and challenges. Eng. Life Sci. 19, 279–291. https://doi.org/10.1002/elsc.201800158
Roy, S., Kim, H.C., Panicker, P.S., Rhim, J.W., Kim, J., 2021. Cellulose nanofiber-based nanocomposite films reinforced with zinc oxide nanorods and grapefruit seed extract. Nanomaterials 11. https://doi.org/10.3390/nano11040877
Sánchez-Gutiérrez, M., Bascón-Villegas, I., Espinosa, E., Carrasco, E., Pérez-Rodríguez, F., Rodríguez, A., 2021. Cellulose nanofibers from olive tree pruning as food packaging additive of a biodegradable film. Foods 10, 1–15. https://doi.org/10.3390/foods10071584
Sánchez-Gutiérrez, M., Espinosa, E., Bascón-Villegas, I., Pérez-Rodríguez, F., Carrasco, E., Rodríguez, A., 2020. Production of cellulose nanofibers from olive tree harvest - A residue with wide applications. Agronomy 10. https://doi.org/10.3390/agronomy10050696
Segal, L., Creely, J.J., Martin, A.E., Conrad, C.M., 1959. An empirical method for estimating the degree of crystallinity of native cellulose using the X-ray diffractometer. Text. Res. J. 29, 786–794. https://doi.org/10.1177/004051755902901003
Singh, R.S., Singh, T., Pandey, A., 2019. Microbial enzymes-an overview. In: Singh, R.S., Singhania, R.R., Pandey, A., Larroche, C. (Eds.), Biomass, Biofuels, Biochemicals: Advances in Enzyme Technology. Elsevier B.V, pp. 1–40. https://doi.org/10.1016/B978-0-444-64114-4.00001-7
Siró, I., Plackett, D., 2010. Microfibrillated cellulose and new nanocomposite materials: a review. Cellulose 17, 459–494. https://doi.org/10.1007/s10570-010-9405-y
Sluiter, A., Hames, B., Ruiz, R., Scarlata, C., Sluiter, J., Templeton, D., Crocker, D., 2012. Determination of structural carbohydrates and lignin in Biomass - NREL/TP-510–42618, Laboratory Analytical Procedure (LAP).
Sluiter, A., Ruiz, R., Scarlata, C., Sluiter, J., Templeton, D., 2008. Determination of extractives in biomass - technical report NREL/TP-510-42619. Lab. Anal. Proced. Colo. https://doi.org/10.1016/j.rmr.2016.02.006
Sorieul, M., Dickson, A., Hill, S.J., Pearson, H., 2016. Plant fibre: Molecular structure and biomechanical properties, of a complex living material, influencing its deconstruction towards a biobased composite. Materials. https://doi.org/10.3390/ma9080618
Sun, J.X., Sun, X.F., Zhao, H., Sun, R.C., 2004. Isolation and characterization of cellulose from sugarcane bagasse. Polym. Degrad. Stab. 84, 331–339. https://doi.org/10.1016/j.polymdegradstab.2004.02.008
Tibolla, H., Pelissari, F.M., Martins, J.T., Vicente, A.A., Menegalli, F.C., 2018. Cellulose nanofibers produced from banana peel by chemical and mechanical treatments: Characterization and cytotoxicity assessment. Food Hydrocoll. 75, 192–201. https://doi.org/10.1016/j.foodhyd.2017.08.027
Tibolla, H., Pelissari, F.M., Menegalli, F.C., 2014. Cellulose nanofibers produced from banana peel by chemical and enzymatic treatment. LWT - Food Sci. Technol. 59, 1311–1318. https://doi.org/10.1016/j.lwt.2014.04.011
United Nations, 2015. Transforming our world: the 2030 Agenda for Sustainable Development [WWW Document]. URL ⟨https://sustainabledevelopment.un.org/post2015/transformingourworld⟩.
Ventura-Cruz, S., Tecante, A., 2019. Extraction and characterization of cellulose nano fi bers from Rose stems (Rosa spp.). Carbohydr. Polym. 220, 53–59. https://doi.org/10.1016/j.carbpol.2019.05.053
Wang, D., Yu, H., Fan, X., Gu, J., Ye, S., Yao, J., Ni, Q., 2018. High aspect ratio carboxylated cellulose nanofibers cross-linked to robust aerogels for superabsorption-flocculants: paving way from nanoscale to macroscale. ACS Appl. Mater. Interfaces 10, 20755–20766. https://doi.org/10.1021/acsami.8b04211
Xing, L., Hu, C., Zhang, W., Guan, L., Gu, J., 2020. Biodegradable cellulose I (II) nanofibrils/poly(vinyl alcohol) composite films with high mechanical properties, improved thermal stability and excellent transparency. Int. J. Biol. Macromol. https://doi.org/10.1016/j.ijbiomac.2020.07.320
Zárate, C.N., Aranguren, M.I., Reboredo, M.M., 2003. Influence of fiber volume fraction and aspect ratio in Resol-Sisal composites. J. Appl. Polym. Sci. 89, 2714–2722. https://doi.org/10.1002/app.12404
Zhu, J.Y., Sabo, R., Luo, X., 2011. Integrated production of nano-fibrillated cellulose and cellulosic biofuel (ethanol) by enzymatic fractionation of wood fibers. Green. Chem. 13, 1339–1344. https://doi.org/10.1039/c1gc15103g